JOURNAL OF MATERIALS SCIENCE 9 (1974) 1911–1916

The influence of brittle boundary layers on the strength of fibrous metallic composites

E. FRIEDRICH, W. POMPE
Zentralinstitut für Festkörperphysik und Werkstofforschung der AdW der DDR, Dresden, GDR

I. M. KOPJOV
Baikov-Institute of Metallurgy an USSR, Moscow, USSR

The brittle boundary layers often caused during the production of composites or by their treatment at higher temperatures, may change the mechanical properties. On the "steel wire/aluminium" system the growth of the intermetallic boundary phase and its influence on the strength of the composite were investigated. Hence followed a maximum strength at small layer thicknesses. By means of fracture investigations new models were developed which allow the calculation of the dependence of strength behaviour on layer thickness.

List of symbols

E_f = Young's modulus of fibre
E_b = Young's modulus of boundary layer
σ_c = external load
σ_f = tensile stress in the fibre
σ_m = tensile stress in the matrix
σ_b = tensile stress in the boundary layer
$\sigma_{uc,f,b}$ = ultimate strength of the composite, the fibre or the boundary layer, respectively
$\bar{\sigma}_f$ = averaged stress in the fibre
τ_{bf} = shear stress in the boundary layer-fibre interface
τ_0 = shear strength of the boundary layer-fibre-interface
ϵ_{uf} = ultimate strain of the fibre
λ = fraction of the layer which has grown into the matrix
β = Weibull parameter
η^{-1} = characteristic length of stress transfer between fibre and boundary layer
d = diameter of the boundary layer
$2l$ = length of the boundary layer segments
r_f = fibre radius
$u(x)$ = displacement field
$v_{f,b,m}$ = volume fraction of fibres, boundary layer or matrix respectively

1. Introduction

The interfaces between the separate components of fibrous composites essentially affect the properties of the composite. For this reason phenomena occurring at the interfaces, especially the growth of boundary layers, are a subject of special interest. Excellent mechanical properties of the composite require a good load transfer between matrix and fibre by means of the boundary layer. In systems of metallic fibres and metallic matrix, boundary layers of usually brittle intermetallic phases are observed. The brittle layers may give rise to microcracks, diminishing the composite strength [1]. This fact entails the question of the optimum thickness of the boundary layer.

The problem of optimum thickness is investigated in the system of steel wire/aluminium matrix. In our investigation we used two types of composites which differed from each other in the parameters of the manufacturing process as well as in the structure (aligned fibres and nets).

2. Experimental results

Our samples were made from Al 99.99 reinforced with 100 μm Mo-maraging steel wire, the latter having a tensile strength of 320 kgf mm^{-2}. Matrix and wire were composed by melt coating. The wire was reduced in hydrogen at 900° C and then drawn through an aluminium melt of 700° C at a rate of 3 m min^{-1}. The procedure resulted in a layer of about 50 μm of aluminium which

corresponds to a volume fraction of 20% fibre. The coated wires were aligned and cut, then hot-pressed in a graphite die at 500 to 600° C for 45 min at a pressure of 0.6×10^3 kgf cm^{-2}. The wires hardened during the process of hot-pressing. The composite plates had a size of $70 \times 10 \times 6$ mm^3.

The tensile strength of the samples was measured on a 10^4 kgf tensile testing machine manufactured by the firm "Zwick". The fracture surfaces were investigated with the help of a scanning electron microscope. The thickness of the boundary layers was determined by means of metallographic techniques. The growth of the diffusion layer Fe_2Al_5 follows a square root law. The temperature dependence of this process can be described by an activation energy of 14 kcal g-at^{-1} (Fig. 1) which coincides well with the data given by Heumann and Dittrich [2]. The layers grow fairly smoothly up to a thickness of about 20 μm (Fig. 2), then in a more irregular and flower-like manner, so that it is no longer possible to speak of a definite thickness.

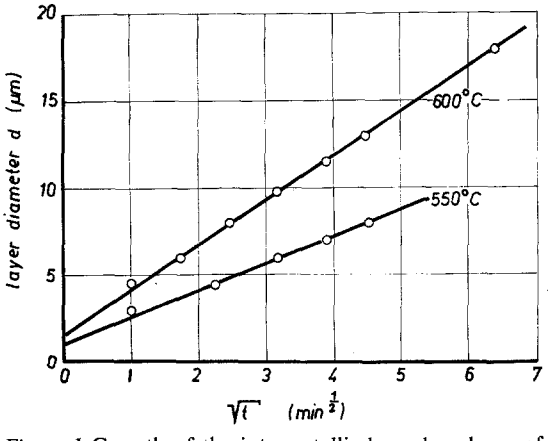

Figure 1 Growth of the intermetallic boundary layer of steel wire/Al-composites in dependence on the hot-pressing time for different temperatures.

The relative strength of the samples is plotted in Fig. 3 as a function of layer thickness d. The real strength of the samples depends on the process parameters of hot-pressing due to the hardening of the wires during this process, and on the volume fraction of fibres. For this reason the observed values of strength of composites with a boundary layer $\sigma_{uc}(d)$ have been normalized to the strength $\sigma_{uc}(d = 0)$, which is to be expected in the case of a composite with an intermediate layer of thickness zero according

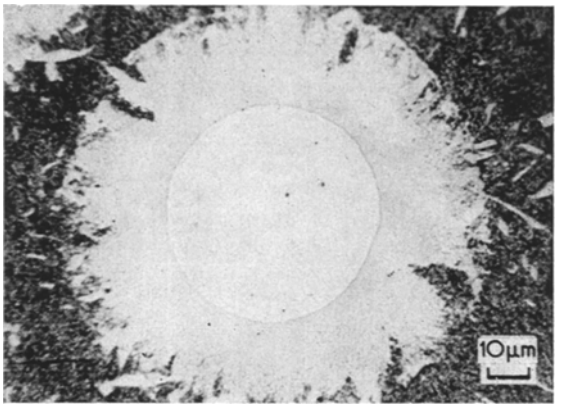

Figure 2 Steel wire/Al-composite sample with intermetallic boundary layer.

to the rule of mixtures. The dots in Fig. 3 represent at least two, in most cases four to six samples.

The strength of the composite has been increased by diffusion layers with a thickness of up to about 6 μm, but with larger values the strength decreased rapidly. The examination by means of the scanning electron microscope revealed the fact that, after rupture, the diffusion layer was broken in numerous segments of nearly identical size (Figs. 4 and 5).

3. Theoretical discussion

In our theoretical investigation we consider the composite as a three-component system: steel, boundary layer, aluminium, without paying any attention to the substructure of the layer. Since the boundary layer is rather brittle, its strength σ_{ub} must be expected to decrease with increasing thickness. This follows from Weibull's theory on the strength of brittle solids:

$$\sigma_{ub} = \sigma_0 \left(\frac{V_0}{V}\right)^{1/\beta} . \qquad (1)$$

Assuming the layer to be cylindrical, we obtain for its volume V

$$V = \pi r_f^2 L v_b / v_f . \qquad (2)$$

The strength of the boundary layer increases with decreasing layer thickness according to Equation 1. Thus there is a critical volume fraction v_b^*, below which the fracture strain of the boundary layer becomes larger than that of the fibres ϵ_{uf}. The critical fraction v_b^* can be obtained from Equations 1 and 2 as

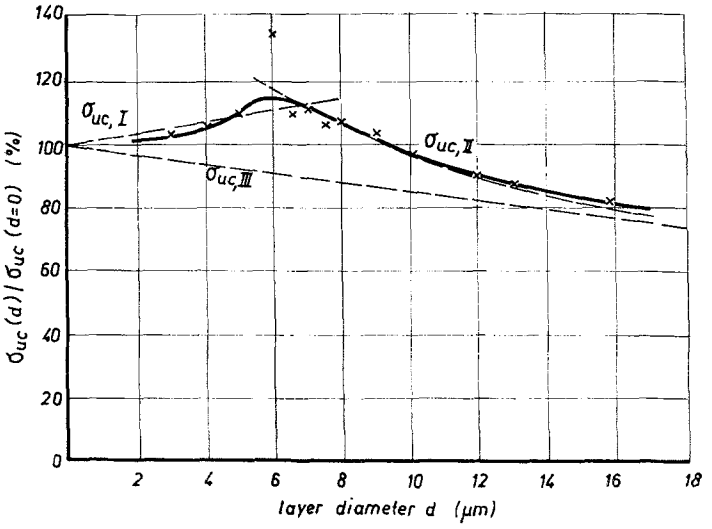

Figure 3 Comparison of the experimentally determined values of the tensile strength $\sigma_{uc}(d)$ in dependence on the layer thickness d with the theoretically calculated values for the various characteristic regions of fracture.

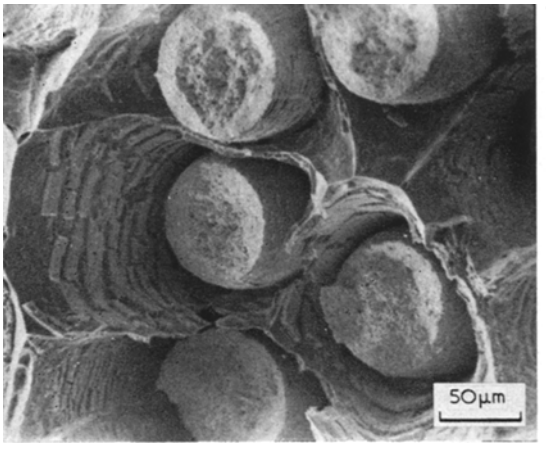

Figure 4

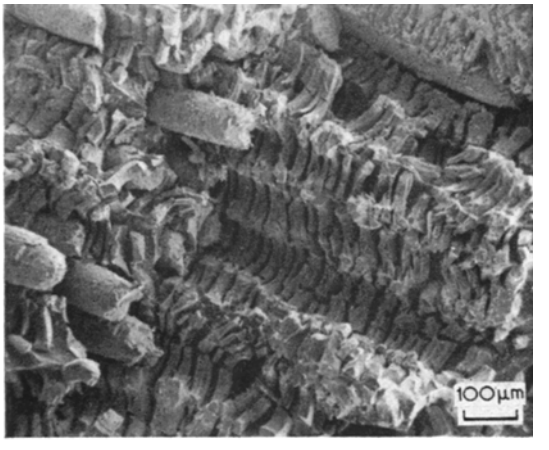

Figure 5

Figures 4 and 5 Scanning-electron-microscopic images of the fracture surfaces of steel/Al-composite samples with intermetallic layer.

$$v_b^* = \frac{V_0 v_f}{L\pi r_f^2}\left(\frac{\sigma_0}{E_b \epsilon_{uf}}\right)^{\beta},$$

As a consequence there are two regions of different fracture behaviour:

(a) $v_b^* > v_b$

In this case fracture is initiated by breaking fibres. The strength of a composite with continuous fibres is given by the expression

$$\sigma_{uc} = v_f\sigma_{uf} + v_b\sigma_b(\epsilon_{uf}) + v_m\sigma_m(\epsilon_{uf}) . \quad (4)$$

If the modulus of the intermetallic compound is higher than that of the matrix we can immediately deduce from Equation 4, that the strength of the composite with diffusion layer ($\sigma_{uc,I}$) is higher than without such a layer ($\sigma_{uc,0}$):

$$\sigma_{uc,I} = \sigma_{uc,0} + v_b\{\lambda[\sigma_b(\epsilon_{uf}) - \sigma_m(\epsilon_{uf})] + (1 - \lambda)[\sigma_b(\epsilon_{uf}) - \sigma_{uf}]\} \quad (5)$$

where λ denotes the percentage of layer volume which has grown into the matrix and, consequently, $1 - \lambda$ the reduction of the wire cross-section.

(b) $v_b > v_b^*$

In this case fracture is initiated within the layer. With increasing load an initial crack within the layer gives rise to one of the following mechanisms:

(1) additional layer cracks;

(2) fracture of fibre caused by stress concentration due to the layer cracks;

(3) debonding of the interface between fibre and intermediate layer caused by shear stress concentration due to the layer crack.

In the case of very thick layers $v_b \gg v_b^*$ mechanism 1 is expected to be the predominant one. Then the layer will desintegrate into segments of the length $2l$, if the load increases. Depending on the shear strength between fibre and layer mechanism 2 or 3 comes into effect: the fibres break due to stress concentration which increases with decreasing length of segments $2l$, or the layer begins to debond. The latter mechanism prevents the segments from breaking down below a minimum length $2l_{min}$.

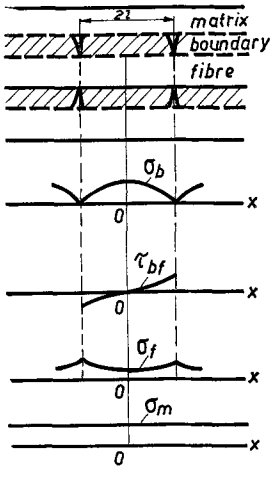

Figure 6 Characteristic stress behaviour within the boundary layer (σ_b), at the interface of fibre and boundary layer (τ_{bf}), within the fibre (σ_f) and within the matrix (σ_m).

Stress concentrations within the matrix can be neglected provided that the matrix should be sufficiently ductile ($\epsilon_m = \bar{\sigma}_f/E_f$). Therefore, we can expect characteristic stress fields as shown in Fig. 6. On the assumption that the matrix ductility should be sufficient, the shear stress τ_{mb} at the interface between matrix and layer is considered to be small as compared to the shear stress τ_0 at the fibre-layer interface. A micro-mechanical analysis (see Appendix) provides an expression for the minimum length of boundary layer segments as follows:

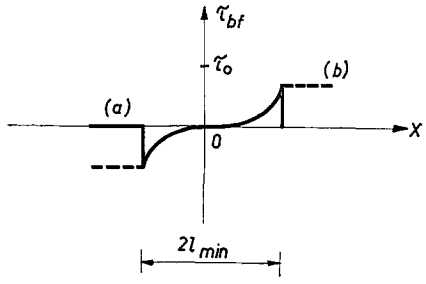

Figure 7 Behaviour of the shear stress τ_{bf} in the fibre boundary layer interface at the beginning of the complete separation (a) and with ideally plastic flow (b) (τ_0 = interface shear strength).

$$l_{min} = \frac{v_b}{v_f}\frac{\sigma_{ub}}{\tau_0}. \tag{6}$$

This result is obtained on the assumption of complete debonding as soon as the shear strength reaches τ_0 (Fig. 7). If the fibre layer interface exhibits an ideally plastic behaviour, i.e. that the shear stress continues to maintain τ_0 after flow has set in, the value of l_{min} decreases by one half.

The rule of mixtures provides a relation between the external load and the stresses in the components:

$$\sigma_c = v_f\bar{\sigma}_f + v_b\bar{\sigma}_b + v_m\bar{\sigma}_m. \tag{7}$$

The stresses $\bar{\sigma}_f$, $\bar{\sigma}_b$ and $\bar{\sigma}_m$ are average values along the fibre. In the case of $v_b \gtrsim v_b^*$ the segments caused by boundary layer cracks are of considerable length, that they do not affect the macroscopic behaviour very much. With increasing thickness, d, or decreasing length of the segments, the stress concentrations increase at their ends. As a result the fibres may break due to overloading. In this case the composite strength decreases with increasing v_b (see Appendix).

$$\sigma_{uc,II} = v_f\sigma_{uf} + v_b(E_b/E_f)\sigma_{uf}\cdot \left[\frac{1 - (\tan h\eta l/\eta l)}{1 + (v_bE_b/v_fE_f)\,(\tan h\eta l/\eta l)}\right] + v_m\sigma_m(\epsilon_{uf}) \tag{8}$$

ηl denoting a characteristic length of our micro-mechanical model which increases with v_b.

As soon as the segments have broken down to the limit $2l_{min}$, debonding of the fibre and layer begins, the stress concentrations at the ends of the

segments vanishing partially. In the case of complete debonding we get a resulting strength as follows:

$$\sigma_{uc,III} = v_f\sigma_{uf} + v_m\sigma_m(\epsilon_{uf}) \qquad (9)$$

i.e. the composite has been weakened due to the complete failure of the diffusion layer. Thus we get a plot of the theoretical composite strength versus layer thickness as shown in Fig. 3. Experimental data on composites of aligned high-strength steel wires and aluminium matrix comply surprisingly well with our theory, if the Young's modulus of the layer is assumed to be $E_b = 12\,000$ kgf mm^{-2}. This value is very close to that of the Fe_2Al_5 phase which is supposed to be the main constituent of the layer.

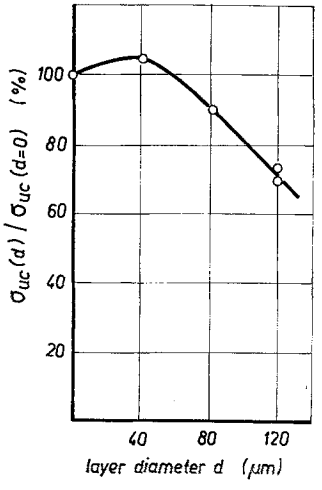

Figure 8 Strength of Cr–Ni–steel wire network/Al-composite $\sigma_{uc}(d)$ in dependence on the thickness d of the intermetallic boundary layer.

Despite of different manufacturing techniques and layer growth conditions the composites of steel net and aluminium qualitatively show the same behaviour (Fig. 8). In view of the sparse information available about the real structure of the layer and the so far limited amount of experimental strength data, quantitative investigations might be unjustified.

Mention should be made that according to our theoretical model, which includes a brittle layer containing microdefects in statistical distribution, the site of the strength maximum (near $v = v_b^*$) depends essentially on the distribution of defects and, as a consequence, on the growth process of the layer. Different conditions (temperature, pressure) result necessarily in different values v_b^* and, therefore, different sites of the maximum. Furthermore v_b^* is affected by the fracture strain of the fibres. Small fracture strains with given fracture strength (high-strength steel wires) result in large v_b^*, i.e. there is a large region where the boundary layer acts as a strengthening component of the composite.

Appendix. Micro-mechanical model for stress transfer in the composite system of fibre/boundary layer/matrix

With the restricting assumptions in Section 3 the problem reduces to the calculation of the shear stress at the fibre boundary-layer interface τ_{bf}, the tensile stress of the layer σ_b and the fibre σ_f.

For the tensile stress the rule of mixtures is put up. In this case stress concentrations are taken into consideration only in the fibre and in the boundary layer [$\epsilon_f = \epsilon_f(x) \neq \epsilon_b(x)$], whereas, with the ductile matrix, only a deformation of $\bar{\epsilon}_m = \bar{\epsilon}_f/E_f$ averaged along the characteristic segment length $2l$ (Fig. 6) is stated.

$$\sigma_c = v_f\sigma_f[\epsilon_f(x)] + v_b\sigma_b[\epsilon_b(x)] + v_m\sigma_m(\bar{\sigma}_f/E_f)\,. \qquad (A1)$$

For the different deformations occurring in the fibre and the matrix, it is possible to approximately derive the following relation, shear stresses between the boundary layer and the matrix being neglected.

$$\frac{d\sigma_b}{dx} + \frac{2v_f}{v_b r_f}\tau_{bf} = 0\,, \quad \frac{d\sigma_b}{dx} = -\frac{v_f}{v_b}\frac{d\sigma_f}{dx}\,. \qquad (A2)$$

Analoguous to the models of Cox and Rosen [3, 4] we state approximately

$$\tau_{bf} = K(u_f - u_b) \qquad (A3)$$

i.e. τ_{bf} is proportional to the displacement of the layer u_b relative to the fibre u_f. Inserting Equation A3 into Equation A2 we get a differential equation

$$\frac{d^2\tau_{bf}}{dx^2} - \eta^2\tau_{bf} = 0\,, \quad \eta^2 = \frac{2v_f}{v_b}K\left(\frac{1+\alpha}{E_b r_f}\right), \quad \alpha = \frac{v_b E_b}{v_f E_f}\,. \qquad (A4)$$

Hence, it follows that there are two regions with different types of solution. Whereas the layer keeps adhering to the fibre with small load (large segments, region I), debonding begins as soon as

τ_{bf} reaches the interface shear strength τ_0 (region II).

Region I

Simple integration leads to the following expressions for the stresses:

$$\tau_{bf} = \tau^* \frac{\sin h\eta x}{\sin h\eta l}$$

$$\sigma_b = \frac{2v_f}{v_b} \frac{\tau^*}{\eta r_f} \frac{(\cos h\eta l - \cos h\eta x)}{\sin h\eta l} \tag{A5}$$

$$\sigma_f = \frac{2\tau^*}{\eta r_f}\left[\frac{\cos h\eta x}{\sin h\eta l} + \frac{1}{\alpha}\cot h\eta l\right] \cdot$$

Using

$$\bar{\sigma}_f = \frac{2\tau^*}{\eta r_f}\left[\frac{1}{\eta l} + \frac{1}{\alpha}\cot h\eta l\right] \tag{A6}$$

for the mean fibre load we get a relation for the external load

$$\sigma_c = v_f\left(\frac{1+\alpha}{1+\alpha \tan h\eta l/\eta l}\right)\bar{\sigma}_f + v_m\sigma_m\left(\frac{\bar{\sigma}_f}{E_f}\right) \tag{A7}$$

which can be used to determine the integration constant τ^*. Debonding begins as soon as the shear stress for $\sigma_b(x = 0) = \sigma_{ub}$ reaches $\tau_{bf}(x = \pm 1) = \tau_0$.

Region II

On the assumption of partially debonding (over the length $l - g$) we get similar relations in the region $0 < |x| < l - g$ as in Equation 5. The case of completely debonding, as shown in Fig. 7, is applied to the remaining region $l - g < |x| < l$. Thus we get a relation between the overall load, the mean fibre load, and the length debonded $l - g$.

$$\sigma_c = v_f\bar{\sigma}_f + v_m\sigma_m(\bar{\sigma}_f/E_f) + v_f\frac{2\tau_0}{\eta r_f}\left(\frac{\eta g \cot h\eta g - 1}{\eta l}\right) \tag{A8}$$

$$\bar{\sigma}_f = \frac{2\tau_0}{\eta r_f}\left[\frac{1}{\eta l} + \frac{1}{\alpha}\cot h\eta g + \frac{l-g}{g}\cot h\eta g\right] \cdot$$

The additional load of the fibres due to the layer at the sites $x = \pm 1$ is diminished by debonding. $\sigma_f(x = \pm 1) =$

$$\frac{1+\alpha}{1+\alpha\left(1 - g/l + \frac{\tan \eta g}{\eta l}\right)}\bar{\sigma}_f \cdot \tag{A9}$$

These solutions of the mathematical model allow one to immediately derive the approximate expressions for the above mentioned composite strength. In the case of $v_b < v_b^*$ the rule of mixtures is valid in connection with $\epsilon_f = \epsilon_b = \epsilon_m$; as soon as fibre fracture begins we can immediately derive from it Equation 5. For $v_b > v_b^*$ we get the more complicated Equations A7 and A8. Equation 8 describing the case of large layer segments, is obtained by inserting $\bar{\sigma}_f = \sigma_{uf}$ into Equation A7. In the case of very small layer segments or of debonding we get a lower strength boundary $\sigma_{uc,III}$ according to Equation 9 by inserting $\bar{\sigma}_f = \sigma_{uf}$ into Equation A8 and approaching the limit $g \to 0$.

References

1. L. M. USTINOV, *Fizika i Chimia Obrabotkij Materialov* 6 (1971) 75.
2. T. HEUMANN and S. DITTRICH, *Z. Metallk.* 44 (1953) 4, S. 154-160.
3. H. L. COX, *Brit. J. Appl. Phys.* 3 (1952) 72.
4. B. ROSEN, "Mechanics of Composite Strengthening", (American Society for Metals, Metals Park, Ohio, 1965) S. 37-75.

Received 26 September 1973 and accepted 7 May 1974.